Angewandte Zuschriften

Metal Nanoparticles

DOI: 10.1002/ange.201107822

Anti-Galvanic Reduction of Thiolate-Protected Gold and Silver Nanoparticles**

Zhikun Wu*

Among the many techniques to engineer the compositions, structures, and properties of metal nanostructures, galvanic reduction (GR) received particular interest owing to its high tunability and feasibility, in particular the possibility to mechanistically study the properties of nanostructures.[1,2] GR occurs spontaneously when the atoms of one metal touch ions of another metal that has a higher electrochemical potential in solution. The metal atoms are oxidized and enter the solution phase, while the metal ions are reduced and deposited on the surface of the metal template, in simple terms, metals can reduce less reactive (or more noble) metal ions in solution. This simple reaction can be used with a wide variety of metal templates and salt precursors, thus providing a straightforward and versatile route to access a broad range of nanostructures (including simple and complex nanostructures).[3–9] However, the opposite of GR (anti-galvanic reduction, AGR), that is, metal ions are reduced by less reactive (or more noble) metals, is not recognized. Recently, Murray and co-workers revealed that a well-studied gold nanocluster, $[Au_{25}(SC_2H_4Ph)_{18}]$, can react with silver ions,[10] thus suggesting that AGR could occur. It is well-known that Au_{25} has multiple charge states, even the anionic and neutral species were unambiguously confirmed by single-crystal X-ray diffraction analyses.[11,12] To exclude the possibility that anionic $[Au_{25}(SC_2H_4Ph)_{18}]$ has a particular reducing ability, the reaction of neutral $[Au_{25}(SC_2H_4Ph)_{18}]$ with silver ions was tried. Furthermore, such replacement on several gold and silver nanoparticles of different sizes was also investigated. The positive results demonstrate the definite occurrence of AGR for small nanoparticles that are protected by thiolates, and these interesting results are presented herein.

First, the reaction product of the reaction between neutral $[Au_{25}(SC_2H_4Ph)_{18}]$ and silver ions was investigated by laser desorption and ionization (i.e. no matrix, LDI) mass spectrometry. In mass spectra of Au_{25} the most abundant species detected is $[Au_{25}S_{12}]^-$(author note: the charge state of gaseous ion is -1).[13] However, for the product of the reaction of $[Au_{25}(SC_2H_4Ph)_{18}]$ with 9.0 equivalents Ag^+, the mass spectra show that bimetal cluster ions, such as $[Au_{22}Ag_3S_{12}]^-$ and $[Au_{23}Ag_2S_{12}]^-$ instead of $[Au_{25}S_{12}]^-$, are abundant species in the mass range from 4000 to 7000 Da, and the comparison of experimental and theoretical isotopic patterns also confirms the assignment of bimetal cluster ions (Figures 1 A–C), thus indicating that the replacement between the silver ions and neutral Au_{25} occurs. X-ray photoelectron spectroscopy (XPS, Figure 1 D) further confirms such reduction: the binding energies of 368.2 (assigned to $Ag3d_{5/2}$) and 374.2 eV (assigned to $Ag3d_{3/2}$) match very well that of pure silver ($Ag3d_{5/2}$: 368.2; $Ag3d_{3/2}$: 374.2 eV). Gold is less reactive (or more noble) than silver, deduced from the electrochemical potential, and it is anticipated that silver metal can reduce gold(III) ions, but the reduction of silver ions by gold metal is difficult in ambient environment according to the galvanic theory. Indeed it was found that silver ions were reduced by Au_{25}, and the gold atoms in Au_{25} were replaced by silver. Such a finding is very surprising, because it is against the classic galvanic theory and was rarely reported before. For convenience, this reaction was named anti-galvanic reduction (AGR). To exclude the possibility that the ability to undergo AGR is a unique property of Au_{25}, the reactions of approximately 2 and 3 nm sized gold nanoparticles with silver ions were also investigated. The approximately 2 nm sized nanoparticles were separated from the residual in the synthesis of Au_{25}, and the approximately 3 nm sized nanoparticles were synthesized by a modified Brust method[14] (for details see the Experimental Section). Note that the approximately 2 nm sized nanoparticles do not show the plasma resonance absorption, whereas the approximately 3 nm sized nanoparticles start to exhibit the plasma peak less prominent than approximately 4 nm sized or even bigger nanoparticles; see Figure 2 C and our previous work[15] for a comparison. After the approximately 2 and 3 nm sized nanoparticles were treated with silver nitrate in a similar way as Au_{25} was treated, silver was detected by XPS (see Figure 2 D). The Au/Ag atom ratios indicated by XPS analyses are 7.0:1 in the case of the approximately 2 nm sized Au nanoparticles and 5.3:1 in the case of the approximately 3 nm sized Au nanoparticles (the starting nanoparticles/$AgNO_3$ weight ratios were both 5.2:1). The binding energies of 368.2 and 374.2 eV (assigned to $Ag3d_{5/2}$ and $Ag3d_{3/2}$, respectively) indicate that the incorporated silver is neutral, that is, the silver ions can be reduced by approximately 2 or 3 nm sized gold nanoparticles as well, which again demonstrates the occurence of AGR. To further test the universality, the approximately 3 nm sized silver nanoparticles that have the same protecting ligand, phenylethanethiolate, were tested. The nanoparticles were obtained by a method similar to that for the synthesis of $[Au_{25}(SC_2H_4Ph)_{18}]$[16] (note: the unstability of silver nanoclusters results in their growth to approximately 3 nm).

---

[*] Prof. Dr. Z. Wu
Key Laboratory of Materials Physics
Anhui Key Laboratory of Nanomaterials and Nanotechnology
Institute of Solid State Physics, Chinese Academy of Sciences
Hefei 230031 (P.R. China)
E-mail: zkwu@issp.ac.cn

[**] This work is supported by the Hundred Talent Program of the Chinese Academy of Sciences and the Natural Science Foundation of China (Grant no. 21171170).

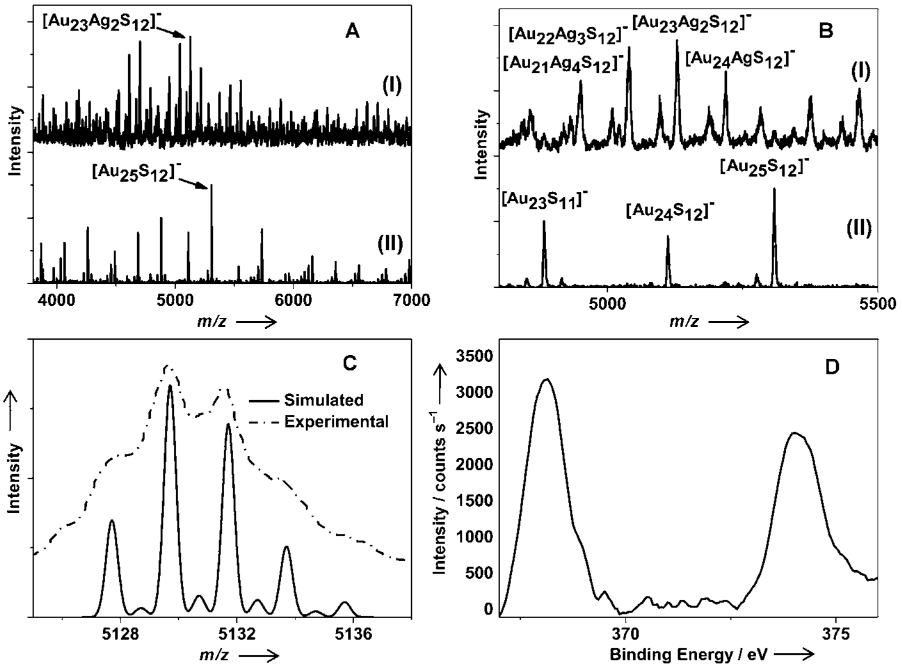

Figure 1. A) Comparison of mass spectra of compounds I and II, and B) magnification of a region of these spectra. C) Comparison of experimental and theoretical isotopic patterns of $[Au_{23}Ag_2S_{12}]^-$. D) Ag3d XPS spectrum of compound II. Note: compound I: $[Au_{25}(SC_2H_4Ph)_{18}]^0$ treated with 9.0 equiv Ag^+; compound II: $[Au_{25}(SC_2H_4Ph)_{18}]^0$.

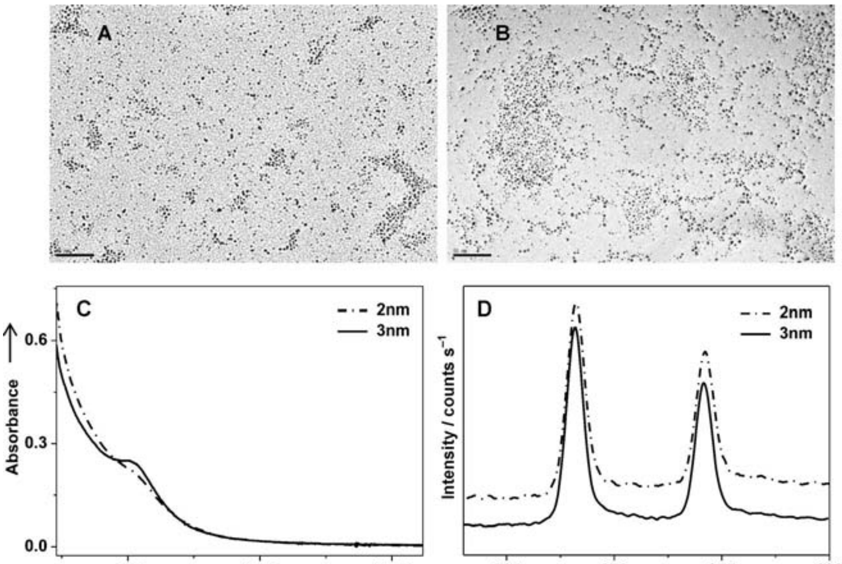

Figure 2. Transmission electron microscopy (TEM) image of A) ca. 2 nm Au nanoparticles and B) ca. 3 nm Au nanoparticles (the scale bar is 50 nm). C) Absorption spectra of ca. 2 and 3 nm sized Au nanoparticles. D) Ag3d XPS spectra of ca. 2 and 3 nm sized Au nanoparticles with incorporated silver(0) (the graphs were shifted and enlarged for clarity).

The silver nanoparticles show an obvious plasma peak at approximately 450 nm (Figure 3 A). After having reacted with copper nitrate completely, silver nanoparticles were precipitated by addition of an excess amount of MeOH. The precipitates were collected and washed thoroughly with MeOH and then dried. XPS analyses show that copper is doped into the silver nanoparticles, and the Ag/Cu atom ratio is 8.6:1 (the starting nanoparticles/Cu-$(NO_3)_2\cdot 3H_2O$ weight ratio was 7.1:1). The binding energy of 932.6 eV, which is assigned to $Cu2p_{3/2}$, indicates that the incorporated copper is neutral (that of $Cu2p_{3/2}$ for pure copper: 932.6 eV); see Figure 3 B. The fact that copper ions can be reduced by more noble silver further demonstrates the universality of AGR. The occurrence of such a reaction is probably attributed to the enhanced reducing ability when the metal size is greatly decreased. Some unexpected properties including catalytic,[17–20] optical,[21–25] electrical,[24,25]structural,[15,26,27] magnetic,[15,28] and melting properties[29] derived from the quantum size effects of metal nanoparticles have been reported and are mostly strongly expressed below approximately 3 nm. Referring to possible applications based on the quantum confinement of electrons, particles in that size region received most attention in the past two decades, which also promoted the study of a novel class of materials, namely thiolate-protected (or thiolated) gold nanoclusters.[30–42] It should be noted that the thiolate ligand on the nanoparticle surface might play an important role in AGR. As is well-known, a thiol ligand will gain partial negative charge after attachment to gold and silver nanoparticle surfaces. Such a partial negative charge from the ligand could be important to assist the reduction of less noble ions, such as Ag^+ and Cu^{2+}. On the other hand, the highly reactive metal atoms on the nanoparticle surface could also be involved in the AGR as a catalyst. The detailed mechanism study needs to be carefully conducted in the near future.

To evaluate the reducing ability, the AGR of Au_{25} (Au_{25} as a representative of gold nanoparticles smaller than approximately 3 nm owing to the well-defined structure and composition) with several other metal ions (including Cu^{2+}, Pb^{2+}, Ni^{2+}, and Fe^{2+}) was investigated. XPS analyses show the incorporation of copper into Au_{25}, and the Au/Cu atom ratio is 17.8:1, far larger than the starting Au/Cu atom ratio 2.8:1 before the reaction. The binding energy 932.4 eV (Figure 4 A, assigned to $Cu2p_{3/2}$) is

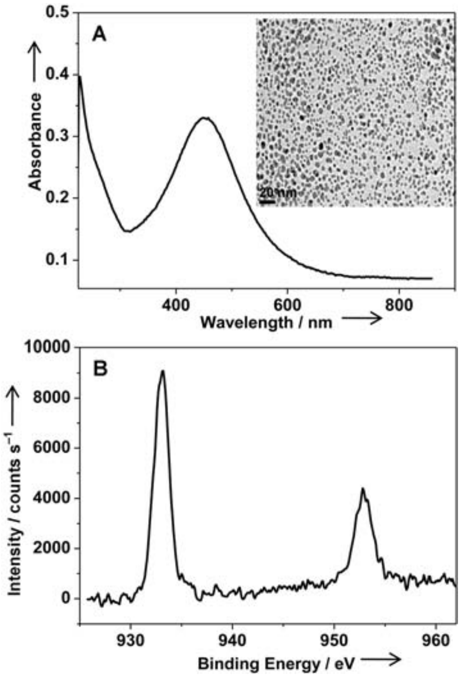

Figure 3. A) Absorption spectrum of ca. 3 nm sized Ag nanoparticles (the inset is a TEM image of Ag nanoparticles, the scale bar is 20 nm). B) Cu2p XPS spectrum of ca. 3 nm sized Ag nanoparticles (treated with $Cu(NO_3)_2$).

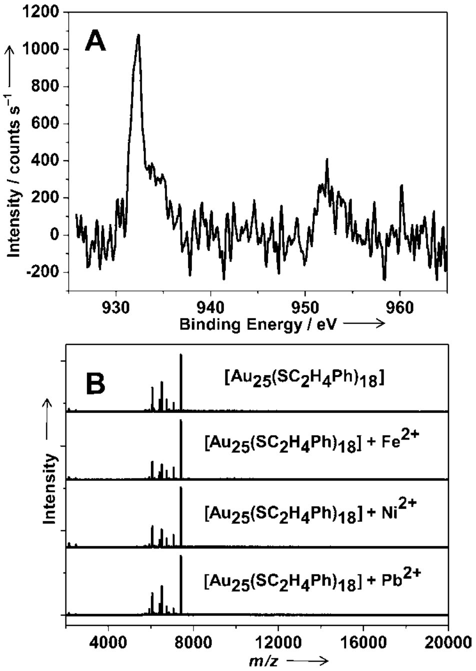

Figure 4. A) Cu2p XPS spectrum of $[Au_{25}(SC_2H_4Ph)_{18}]$ (treated with $Cu(NO_3)_2$). B) MS spectra of pure $[Au_{25}(SC_2H_4Ph)_{18}]$ and $[Au_{25}(SC_2H_4Ph)_{18}]$ treated with different cations (Fe^{2+}, Ni^{2+}, Pb^{2+}; spectra acquired in positive ionization mode).

close to that in pure Cu (932.6 eV), essentially different from that in $Cu(NO_3)_2$ ($Cu2p_{3/2}$: 935.5 eV). Those facts indicate that the incorporated copper exists in neutral charge state. However, incorporation of the other three metals could not be detected by XPS, and matrix-assisted laser desorption/ionization time of flight mass spectrometry (MALDI-TOF MS) also did not detect Pb-, Ni-, or Fe-doped Au_{25} (see Figure 3), thus indicating that Au_{25} is inert to these metal cations owing to the limited reducing activity. But it is still surprising to find that gold of sizes up to 3 nm can reduce copper ions, or in other words, that it can be even more reactive than copper (in bulk). Thus, the reactivity series of the above mentioned metals can be arranged as Fe > Ni > Pb > Au (up to ca. 3 nm size) > Cu > Ag (other metals are in bulk) in order of decreasing reactivity.

We found that when the size of gold or silver particles (may be extended to other metals) is decreased to less than approximately 3 nm, the reducing activity is greatly strengthened: they can reduce some more reactive or less noble metal ions (for example, reduce Cu^{2+} to Cu^0). This finding is significant, because: 1) it is somehow opposite to the classic galvanic theory, which says that metal ions can be readily reduced by more reactive metals, whereas the other way is difficult in ambient environment owing to the negative driving force; 2) anti-galvanic reduction could provide a facile and mild method to make alloys on the nanoscale or tune the compositions, structures, and properties of nanostructures that are otherwise difficult to obtain.

Experimental Section

Chemicals: Hydrogen tetrachloroaurate hydrate ($HAuCl_4{\cdot}4H_2O$, $\geq 99.9\%$, Shanghai Chemical Reagent Co. LTD), copper nitrate trihydrate ($Cu(NO_3)_2{\cdot}3H_2O$, $\geq 99.5\%$, Shanghai Jinghua Scientific & Technological Research Institute), nickel(II) nitrate hexahydrate ($Ni(NO_3)_2{\cdot}6H_2O$, $\geq 98.0\%$, Hanson Shanghai Chemical Reagent Co., Ltd), toluene (C_7H_8, $\geq 99.5\%$, Xilong chemical), tetraoctylammonium bromide ($(C_8H_{17})_4NBr$, 98%, Aladdin), phenylethyl mercaptan (PhC_2H_4SH, $\geq 99\%$, Aldrich), silver nitrate ($AgNO_3$, $\geq 99.8\%$) and lead nitrate ($Pb(NO_3)_2$, $\geq 99.0\%$) were purchased from Tianjin Guangfu Fine Chemical Research Institute, sodium borohydride ($NaBH_4$, $\geq 96\%$), tetrahydrofuran (C_4H_8O, $\geq 99.9\%$), acetonitrile (CH_3CN, $\geq 99.0\%$), ethanol (EtOH, $\geq 99.7\%$), dichloromethane (CH_2Cl_2, $\geq 99.5\%$), and methanol (CH_3OH, $\geq 99.5\%$) were purchased from Sinopharm Chemical Reagent Co. Ltd.

All chemicals were used as received except THF, through which N_2 was bubbled. Nanopure water (resistivity 18.2 MΩcm) was produced with a Milli-Q NANO pure water system.

Synthesis of $[Au_{25}(SC_2H_4Ph)_{18}]$ and ca. 2 nm sized gold nanoparticles: $[Au_{25}(SC_2H_4Ph)_{18}]$ and ca. 2 nm sized gold nanoparticles were synhesized according to a modified reported method.[16] Tetraoctylammonium bromide (TOABr, 525.0 mg, 0.96 mmol) and $HAuCl_4{\cdot}4H_2O$ (387.5 mg, 0.94 mmol) were dissolved in THF (24.0 mL) in a three-necked flask, and the resulting solution was cooled to 0 °C in an ice bath over a period of 30 min. $PhCH_2CH_2SH$ (650 μL, 5 equivalents per mole of gold) was slowly added to the flask. After the solution turned clear over a period of ca. 2.5 h, an aqueous solution of $NaBH_4$ (409.3 mg, 11.5 equivalents per mole of gold, freshly dissolved in 8.0 mL ice-cold nanopure water) was rapidly added at once under vigorous stirring. The reaction was allowed to proceed under constant stirring for ca. four hours. After removal of the water layer, a large amount of cold water (ca. 70 mL) was added, the precipitates were collected and thoroughly washed with water and MeOH, then dried under reduced pressure at room temperature, and CH_3CN was added to the dried product to extract $[Au_{25}(SC_2H_4Ph)_{18}]$. Approximately 2 nm sized gold nanoparticles were obtained from the left residual after the Au_{25} was extracted. The purities of $[Au_{25}(SC_2H_4Ph)_{18}]^-$ and ca. 2 nm sized gold nanoparticles were further improved after recrystallizing twice from CH_3CN/MeOH solution and toluene/MeOH solution, respectively. The $[Au_{25}(SC_2H_4Ph)_{18}]^-$ solution (1 mg mL^{-1} in CH_2Cl_2) was converted to neutral $[Au_{25}(SC_2H_4Ph)_{18}]^0$ after stirring overnight.[12b,22b]

Synthesis of ca. 3 nm sized gold nanoparticles**:** Gold nanoparticles of ca. 3 nm were synthesized according to a modified Brust method.[14] $HAuCl_4{\cdot}4\,H_2O$ (419.8 mg, 1.02 mmol, in ca. 1.0 mL EtOH) was added into a toluene solution (25 mL) of TOABr (613.1 mg, 1.10 mmol). After magnetic stirring for ca. 20 min, the dissolution was completed, and the resulting solution was cooled down to ca. 0 °C in an ice bath over a period of 30 min. $PhCH_2CH_2SH$ (71 µL, 0.5 equivalent per mole of gold) was slowly added, and the solution was stirred for ca. 1.5 h. A freshly made aqueous solution of $NaBH_4$ (424.3 mg, dissolved in 12.5 mL ice-cold H_2O) was then added rapidly into the reaction mixture under vigorous stirring. The reaction was stopped after constant stirring for 11 h, the water layer was removed, the toluene layer was washed three times with cold water, filtered, and then transferred to a clean vessel. An adequate amount of MeOH was added into the toluene solution until a large amount of precipitate was found. The solid was collected and washed thoroughly with MeOH and then dried. TEM confirmed there was a narrow distribution and the average size was ca. 3 nm (see Figure 2 B).

Synthesis of ca. 3 nm sized silver nanoparticles: Approximately 3 nm sized silver nanoparticles were synthesized according to the reported one-pot method[16] with some modifications. $AgNO_3$ (248.8 mg, 1.46 mmol) was dissolved in THF (30.0 mL) in a three-necked flask, the resulting solution was cooled to ca. 0 °C in an ice bath over a period of 30 min. $PhCH_2CH_2SH$ (809 µL, 4 equivalents per mole of gold) was slowly added to the flask. Five hours later, an aqueous solution of $NaBH_4$ (556.4 mg, 10.0 equivalents per mole of gold, freshly dissolved in 7.5 mL ice-cold nanopure water) was rapidly added at once under vigorous stirring. The reaction was allowed to proceed under constant stirring for 11 h. After removal of the water layer, a large amount of cold water (ca. 80 mL) was added, the precipitates were collected and thoroughly washed with water and MeOH, then dried under reduced pressure at room temperature. CH_2Cl_2 was added to the dried product, and after the removal of some insoluble solid, an adequate amount of MeOH was added until a large amount of precipitate was formed. The precipitates were collected and dried. TEM confirmed there was a narrow distribution and the average size was ca. 3 nm (see Figure 3 A inset; note: the dense silver nanoparticles can aggregate under the irradiation of the electron beam).

Fabrication of samples for MS and XPS analyses: The samples for MS and XPS analyses were made by the following general protocols: Nanoparticles (ca. 5.0 mg, in ca. 120 µL CH_2Cl_2) were mixed with the designated metal ions (ca. 10 µL in MeOH, in several portions) in the required weight ratios, vortexed for 30 s, incubated for 1.5 h, then an excess of MeOH was added into the reaction mixture until large quantities of precipitates were formed. The precipitates were collected and washed for at least five times with an excess amount of MeOH to remove the free ions, then dried for MS and XPS analyses.

For the silver-doped samples, the weight ratios of nanoparticles (including Au_{25}, ca. 2 and 3 nm Au nanoparticles) with silver nitrate were all 5.2:1; for the copper-doped samples, the weight ratio of Au_{25} to copper nitrate trihydrate was 11.0:1, the weight ratio of ca. 3 nm Ag nanoparticles with copper nitrate trihydrate was 7.1:1; For the reaction of Au_{25} with other metal ions, the Au/M (M: Fe^{2+}, Pb^{2+}, Ni^{2+}) atom ratios of the starting materials were all addjusted to 2.8:1.

Characterization: All UV/Vis/NIR absorption spectra were recorded using a UV3600 spectrophotometer. Mass analyses were performed with a Voyager DE STR time-of-flight (TOF) mass spectrometer, with or without *trans*-2-[3-(4-*tert*-butylphenyl)-2-methyl-2-propenylidene] malononitrile as the matrix. XPS measurements were performed on a Thermo ESCALAB 250 configured with a monochromated $Al_{K\alpha}$ (1486.8 eV) 150 W X-ray source, 0.5 mm circular spot size, a flood gun to counter charging effects, and the analysis chamber base pressure lower than 1×10^{-9} mbar, data were collected with FAT = 20 eV. The takeoff angle, defined as the angle between the substrate normal and the detector, was fixed at 0°. Substrates were mounted on standard sample studs by means of double-sided adhesive tapes. All binding energies were calibrated using either the Au($4f_{7/2}$) peak (84.0 eV) or the C(1 s) carbon peak (284.6 eV). The nanoparticles' sizes (ca. 2 and 3 nm) were determined by TEM (JEOL2010).

Received: November 7, 2011

Keywords: electrochemistry · galvanic reduction · gold · nanoparticles · silver

---

[1] C. M. Cobley, Y. Xia, *Mater. Sci. Eng. R* **2010**, *70*, 44–62.
[2] S. E. Skrabalak, J. Chen, Y. Sun, X. Lu, L. Au, C. M. Cobley, Y. Xia, *Acc. Chem. Res.* **2008**, *41*, 1587–1595.
[3] S. J. Guo, S. J. Dong, E. Wang, *Chem. Eur. J.* **2008**, *14*, 4689–4695.
[4] J. X. Fang, X. N. Ma, H. H. Cai, X. P. Song, B. J. Ding, *Nanotechnology* **2006**, *17*, 5841–5845.
[5] Q. B. Zhang, J. P. Xie, J. Liang, J. Y. Lee, *Adv. Funct. Mater.* **2009**, *19*, 1387–1398.
[6] D. Aherne, M. Gara, J. M. Kelly, Y. K. Gun'ko, *Adv. Funct. Mater.* **2010**, *20*, 1329–1338.
[7] Y. Liu, A. R. Hight Walker, *ACS Nano* **2011**, *5*, 6843–6854.
[8] L. Au, X. M. Lu, Y. N. Xia, *Adv. Mater.* **2008**, *20*, 2517–2522.
[9] E. Skrabalak, L. Au, X. D. Li, Y. Xia, *Nat. Protoc.* **2007**, *2*, 2182–2190.
[10] J.-P. Choi, C. A. Fields-Zinna, R. L. Stiles, R. Balasubramanian, A. D. Douglas, M. C. Crowe, R. W. Murray, *J. Phys. Chem. C* **2010**, *114*, 15890–15896.
[11] M. W. Heaven, A. Dass, P. S. White, K. M. Holt, R. W. Murray, *J. Am. Chem. Soc.* **2008**, *130*, 3754–3755.
[12] a) M. Zhu, C. M. Aikens, F. J. Hollander, G. C. Schatz, R. Jin, *J. Am. Chem. Soc.* **2008**, *130*, 5883–5885; b) M. Zhu, W. T. Eckenhoff, T. Pintauer, R. Jin, *J. Phys. Chem. C* **2008**, *112*, 14221–14224.
[13] a) Z. Wu, C. Gayathri, R. R. Gil, R. Jin, *J. Am. Chem. Soc.* **2009**, *131*, 6535–6542; b) Z. Wu, R. Jin, *ACS Nano* **2009**, *3*, 2036–2042; c) Z. Wu, R. Jin, *Chem. Eur. J.* **2011**, *17*, 13966–13970.
[14] M. Brust, M. Walker, D. Bethell, D. J. Shiffrin, R. Whyman, *J. Chem. Soc. Chem. Commun.* **1994**, 801–802.
[15] Z. Wu, J. Chen, R. Jin, *Adv. Funct. Mater.* **2011**, *21*, 177–183.
[16] Z. Wu, J. Suhan, R. Jin, *J. Mater. Chem.* **2009**, *19*, 622–626.
[17] M. Haruta, T. Kobayashi, H. Sano, N. Yamada, *Chem. Lett.* **1987**, 405–408.
[18] M. Valden, X. Lai, D. W. Goodman, *Science* **1998**, *281*, 1647–1650.
[19] M. D. Hughes, Y.-J. Xu, P. Jenkins, P. McMorn, P. Landon, D. I. Enache, A. F. Carley, G. A. Attard, G. J. Hutchings, F. King, E. H. Stitt, P. Johnston, K. Griffin, C. J. Kiely, *Nature* **2005**, *437*, 1132–1135.
[20] M. Turner, V. B. Golovko, O. P. H. Vaughan, P. Abdulkin, A. Berenguer-Murcia, M. S. Tikhov, B. F. G. Johnson, R. M. Lambert, *Nature* **2008**, *454*, 981–983.
[21] L. A. Peyser, A. E. Vinson, A. P. Bartko, R. M. Dickson, *Science* **2001**, *291*, 103–106.
[22] a) Z. Wu, E. Lanni, W. Chen, M. E. Bier, D. Ly, R. Jin, *J. Am. Chem. Soc.* **2009**, *131*, 16672–16674; b) Z. Wu, R. Jin, *Nano Lett.* **2010**, *10*, 2568.

[23] O. M. Bakr, V. Amendola, C. M. Aikens, W. Wenseleers, R. Li, L. D. Negro, G. C. Schatz, F. Stellacci, *Angew. Chem.* **2009**, *121*, 6035 – 6040; *Angew. Chem. Int. Ed.* **2009**, *48*, 5921 – 5926.

[24] G. Schmid, M. Bäumle, M. Geerkens, I. Heim, C. Osemann, T, Sawitowski, *Chem. Soc. Rev.* **1999**, *28*, 179 – 185.

[25] C. Xu, X. Lai, G. W. Zajac, D. W. Goodman, *Phys. Rev. B* **1997**, *56*, 13464 – 13482.

[26] R. L. Whetten, J. T. Khoury, M. M. Alvarez, S. Murthy, I. Vezmar, Z. L. Wang, P. W. Stephens, C. L. Cleveland, W. D. Luedtke, U. Landman, *Adv. Mater.* **1996**, *8*, 428 – 433.

[27] P. D. Jadzinsky, G. Calero, C. J. Ackerson, D. A. Bushnell, R. D. Kornberg, *Science* **2007**, *318*, 430 – 432.

[28] Y. Volokitin, J. Sinzig, L. J. De Jongh, G. Schmid, M. N. Vargaftik, I. I. Moiseevi, *Nature* **1996**, *384*, 621 – 623.

[29] P. Buffat, J.-P. Borel, *Phys. Rev. A* **1976**, *13*, 2287 – 2298.

[30] T. G. Schaaff, M. N. Shafigullin, J. T. Khoury, I. Vezmar, R. L. Whetten, W. G. Cullen, P. N. First, *J. Phys. Chem. B* **1997**, *101*, 7885 – 7891.

[31] T. G. Schaaff, G. Knight, M. N. Shafigullin, R. F. Borkman, R. L. Whetten, *J. Phys. Chem. B* **1998**, *102*, 10643 – 10646.

[32] M. J. Hostetler, J. E. Wingate, C.-J. Zhong, J. E. Harris, R. W. Vachet, M. R. Clark, J. D. Londono, S. J. Green, J. J. Stokes, G. D. Wignall, G. L. Glish, M. D. Porter, N. D. Evans, R. W. Murray, *Langmuir* **1998**, *14*, 17 – 30.

[33] H. Qian, W. T. Eckenhoff, Y. Zhu, T. Pintauer, R. Jin, *J. Am. Chem. Soc.* **2010**, *132*, 8280 – 8281.

[34] Y. Negishi, K. Nobusada, T. Tsukuda, *J. Am. Chem. Soc.* **2005**, *127*, 5261 – 5270.

[35] N. K. Chaki, Y. Negishi, H. Tsunoyama, Y. Shichibu, T. Tsukuda, *J. Am. Chem. Soc.* **2008**, *130*, 8608 – 8610.

[36] Z. Wu, M. A. MacDonald, J. Chen, P. Zhang, R. Jin, *J. Am. Chem. Soc.* **2011**, *133*, 9670 – 9673.

[37] E. S. Shibu, T. Pradeep, *Chem. Mater.* **2011**, *23*, 989 – 999.

[38] Y. Levi-Kalisman, P. D. Jadzinsky, N. Kalisman, H. Tsunoyama, T. Tsukuda, D. A. Bushnell, R. D. Kornberg, *J. Am. Chem. Soc.* **2011**, *133*, 2976 – 2982.

[39] G. H. Woehrle, M. G. Warner, J. E. Hutchison, *J. Phys. Chem. B* **2002**, *106*, 9979 – 9981.

[40] O. Toikkanen, V. Ruiz, G. Rönnholm, N. Kalkkinen, P. Liljeroth, B. M. Quinn, *J. Am. Chem. Soc.* **2008**, *130*, 11049 – 11055.

[41] A. Dass, *J. Am. Chem. Soc.* **2009**, *131*, 11666 – 11667.

[42] J. Zheng, J. T. Petty, R. M. Dickson, *J. Am. Chem. Soc.* **2003**, *125*, 7780 – 7781.